SCIENTIFIC REPORTS

OPEN

SUBJECT AREAS:
MATERIALS FOR ENERGY AND CATALYSIS
INORGANIC CHEMISTRY
NANOSCALE MATERIALS
CHEMICAL ENGINEERING

Received
20 February 2013

Accepted
31 July 2013

Published
15 August 2013

Correspondence and requests for materials should be addressed to S.S. (s.smart@uq.edu.au)

Tailoring the oxidation state of cobalt through halide functionality in sol-gel silica

Gianni Olguin[1,2], Christelle Yacou[1], Simon Smart[1] & João C. Diniz da Costa[1]

[1]The University of Queensland, FIMLab – Films and Inorganic Membrane Laboratory, School of Chemical Engineering, Brisbane, Qld 4072, Australia, [2]Pontificia Universidad Católica de Valparaíso, Escuela de Ingeniería Química, Valparaíso, Chile.

The functionality or oxidation state of cobalt within a silica matrix can be tailored through the use of cationic surfactants and their halide counter ions during the sol-gel synthesis. Simply by adding surfactant we could significantly increase the amount of cobalt existing as Co_3O_4 within the silica from 44% to 77%, without varying the cobalt precursor concentration. However, once the surfactant to cobalt ratio exceeded 1, further addition resulted in an inhibitory mechanism whereby the altered pyrolysis of the surfactant decreased Co_3O_4 production. These findings have significant implications for the production of cobalt/silica composites where maximizing the functional Co_3O_4 phase remains the goal for a broad range of catalytic, sensing and materials applications.

The silica sol-gel process represents a powerful, and yet a simple approach, to synthesize functional materials for sensors, membranes and optical applications. With the advent of nanotechnology, the field of silica sol-gel has been significantly expanded, as a plethora of ligand and non-ligand templates have been employed as building blocks in the construction of elegant novel molecular structures[1]. Examples include the use of surfactants in the sol-gel process for the formation of micelles leading to hollow spheres[2], or cavities in the silica matrix to tailor molecular size and shape selectivity[3–5], or template carbonization to counteract silica hydro-instability[6]. In recent times, embedding metal oxides in silica matrices has added further functionalities. Of particular importance, cobalt oxide and silica have become one of the most preferred functional composite materials for a broad range of applications including gas reaction catalysis[7] or long-term stability in high temperature gas separation[8], magnetic materials and gas sensors[9–11]. Previous efforts for catalysis have focussed on two-step synthesis procedures wherein a cobalt precursor is loaded into a pre-existing mesoporous silica support by solution impregnation followed by calcination in an oxidising atmosphere[12–15]. Concurrent development in the membrane field, however, utilized a one-pot fabrication technique whereby the cobalt and silica precursors are homogeneously mixed during the sol-gel synthesis[16,17]. In each case, the cobalt existing as an oxide within the silica framework is highly desirable as its functionality is highly dependent on its oxidation state. However, recent reports suggest that only a small to moderate fraction of the cobalt is embedded as a high valence cobalt oxide (Co_3O_4) inside silica or zeolite frameworks[18,19]. Consequently, increasing the yield of Co_3O_4 from the cobalt precursor has been one of the research aims of this field, thereby dictating innovation in fabrication procedures.

In pursuing strategies to leverage further functionalities in silica derived materials, we show a procedure to maximize the formation of Co_3O_4 in porous silica. We report here for the first time that the oxidation state of cobalt within a silica matrix can actually be controlled through the careful addition of short chain surfactant hexyl triethyl ammonium bromide (HTAB) during the sol-gel synthesis. In particular, we have found that the halide counter ions of the cationic HTAB preferentially coordinate with cobalt ions during the sol-gel synthesis and that this later enhances the oxidation of the cobalt precursors to Co_3O_4 within the silica. This finding is counter-intuitive, as HTAB is generally employed as a pore size tailoring agents to enhance the microporosity of silica[20,21] instead of tailoring the cobalt oxidation state as reported in this work.

Results

FTIR spectra (see Supplementary Fig. S1) of calcined xerogels were deconvoluted and the peak area for Co_3O_4[11] at 670 cm^{-1} was normalized against the peak area of the siloxane bridges[22] at 1080 cm^{-1}. The results in Fig. 1 show Co_3O_4 concentration increasing in the calcined xerogels as a function of the initial surfactant content, reaching a maximum at a surfactant/cobalt molar ratio of $x \sim 1$. These results appear inconsistent with the initial sol-gel

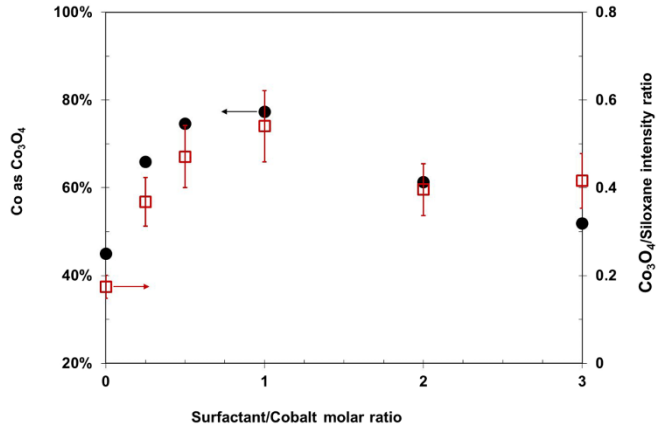

Figure 1 | Cobalt oxide variation with surfactant concentration in the calcined samples. Percentage of Co as Co_3O_4 (●) from XPS analysis. Ratio of peak areas for Co_3O_4 to siloxane bonds from FTIR analysis (□). Error bars represent an interval of 95% standard confidence.

preparation where the concentration of the cobalt precursor was kept constant for all samples and no precipitation or phase separation was observed. Importantly, no cobalt silicate[23] was observed at 860 cm^{-1}, indicating that the cobalt exists within all samples as either Co_3O_4 or Co^{2+} which is undetectable to FTIR. Transmission electron microscopy showed that the Co_3O_4 particles varied in size between 20 and 75 nm were embedded in the silica matrix, with an average particle size of 40 nm (see Supplementary Information Fig. S2). X-ray diffraction measurements exhibits patterns assigned to Co_3O_4 (see Supplementary Information Fig. S3). Using Scherrer's equation, the average crystal size was calculated at 32 nm (see Supplementary Information Table S1). In order to confirm both the absence of cobalt silicate and the presence of Co^{2+} and to actually quantify the yield of Co_3O_4, further analysis of the cobalt oxidation states was also undertaken via XPS. Corresponding high resolution XPS spectra of the Co 2p regions can be found in the supplementary information (see Supplementary Fig. S4) which confirmed the above hypothesis. Similarly to FTIR, XPS results (also in Fig. 1) clearly show that amount of cobalt present in the tetroxide form[24,25], increases from 44% to 77% for $0 < x < 1$, and then reverses its effect thereafter. Therefore, both FTIR and XPS results clearly indicate that the HTAB surfactant is changing the oxidation state of cobalt oxide embedded in the silica matrix.

The cobalt oxidation functionality attained by the HTAB surfactant that we uncovered in this work has not been previously reported. We postulate that the underlying mechanism of the enhanced Co_3O_4 functionality lies in the complexation of the cobalt ions with the HTAB surfactant during the sol-gel synthesis. Typical cobalt silica sols possess the distinctive red-pink color associated with the octahedral form of the Co^{2+} ion in aqueous solution[11]. In contrast, the addition of HTAB to generate the hybrid surfactant/cobalt silica sols resulted in a distinct color change to cobalt blue, which is characteristic of the tetrahedral form of the Co^{2+} ion. The vibrancy of the blue (see Supplementary Fig. S5) is indicative of coordination of the cobalt ions with a weak halide ligand such as bromide[26]. These cobalt-halide (e.g. bromide) complexes form preferentially in solvents that are less polar than water[27,28], as is the case with our silica sol-gel recipes. This visual evidence was confirmed through DR-UV-Vis of the dried xerogels (see Supplementary Fig. S6), which additionally indicates that the drying process does not disrupt the cobalt bromide complex within the silica matrix. This is in contrast to native cobalt silica where the cobalt ions are strongly coordinated with silanol groups or siloxane bridges even after drying[19].

Upon reaching a maximum Co_3O_4 formation at $x \sim 1$, further HTAB addition beyond this point started inhibiting the yield of Co_3O_4. Underpinning this reverse mechanism is the interaction between silica, HTAB and the cobalt oxide particle, evidenced by the subtle change in the nitrogen adsorption isotherms (see Supplementary Fig. S7) and differential thermal analysis (DTA). The samples prepared with surfactant/cobalt ratios of $x < 1$ were highly microporous materials characterized by type I isotherms. However, when $x > 1$, capillary condensation was observed in the nitrogen isotherms, clearly indicating that excess surfactant lead to the formation of mesopores in the cobalt oxide silica network. DTA analysis in Fig. 2 reveals that the samples prepared with $x = 0.5$ exhibited a narrow exothermic peak at ~250°C typically associated with the combustion of the HTAB embedded in silica matrices[29]. However, for the samples prepared with $x > 1$, the peak at ~250°C is less intense, whilst a second exothermic peak appeared at ~535°C, which is contrary to the endothermic region for the samples prepared with $x < 1$. This result is incongruous with the expected surfactant/silica interactions. Whilst it is clear from the adsorption isotherms that some of the excess surfactant ($x > 1$) is generating mesoporous structures, if all the excess surfactant lead to the formation of proto-micelles and or further interact with the silica surface, then we would expect the intensity of exothermic peak at ~250°C to be stronger than the sample $x = 0.5$. However, this is not the case, thus suggesting that the silica surface saturation has been reached and the excess surfactant is playing an additional role.

To shed more light on the nature of the excess surfactant interaction, TGA-MS of the calcination process was carried out for the sample with largest amount of surfactant ($x = 3$). The results in Fig. 3 clearly show CO_2, NO_2 and Br leaving the silica matrix above 500°C, which perfectly matches with the secondary exothermic peak at ~535°C observed through DTA (Fig. 2). These observations indicate

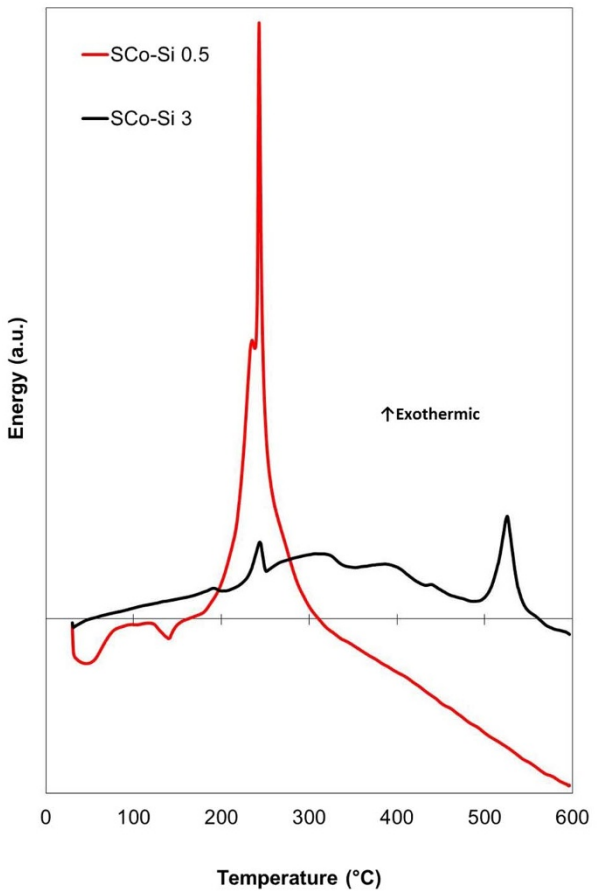

Figure 2 | DTA curves showing the calcination of surfactant cobalt silica samples where $x = 0.5$ (solid red line) and 3 (solid black line).

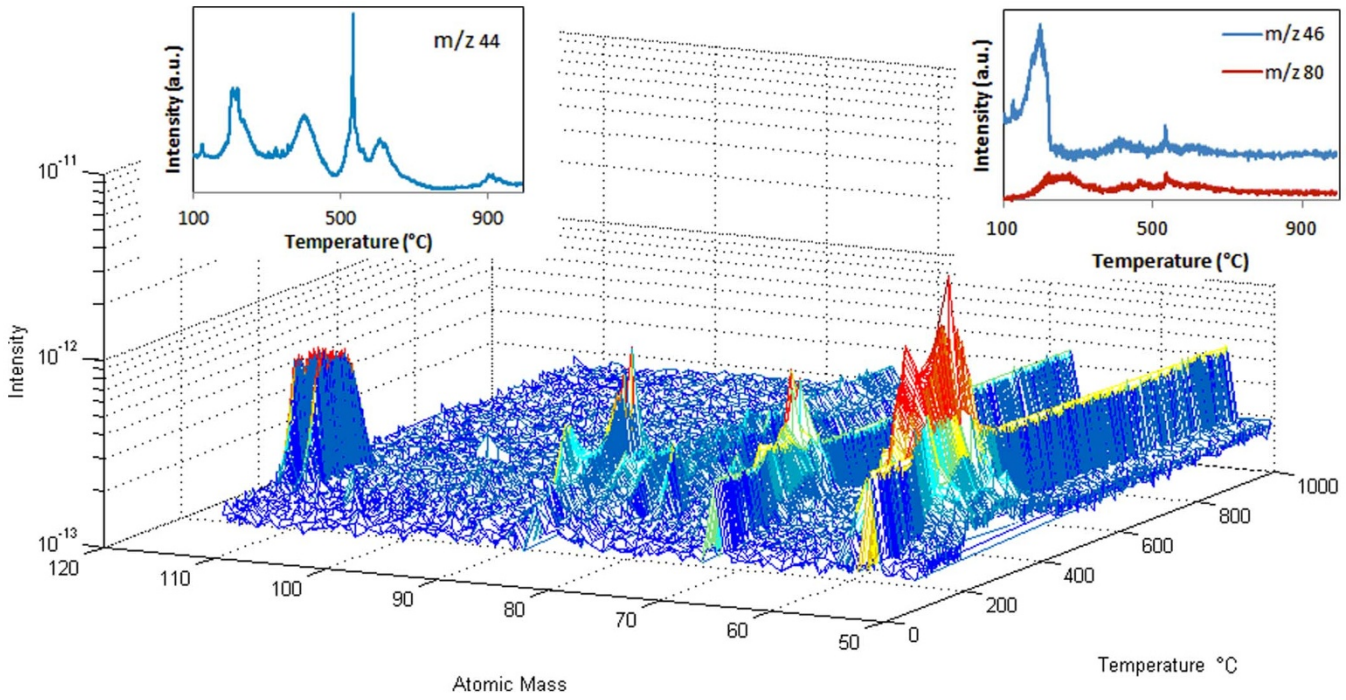

Figure 3 | TGA-MS of SCoSi 3.0 sample. 3D graph depicts the thermal evolution of relevant species with a.m.u. above 50, which leave the matrix from 200 to 450°C in accordance with typical HTAB decomposition process in silica matrices. Aliphatic groups C_4, C_5 and C_6 are observed at 56, 74 and 84 a.m.u. respectively, whilst the ethyl bromide double peak is present at 110 a.m.u. Left inset: CO_2 evolution (m/z = 44) with temperature. Right inset: NO_2 (m/z = 46) and Br (m/z = 80) evolution with temperature.

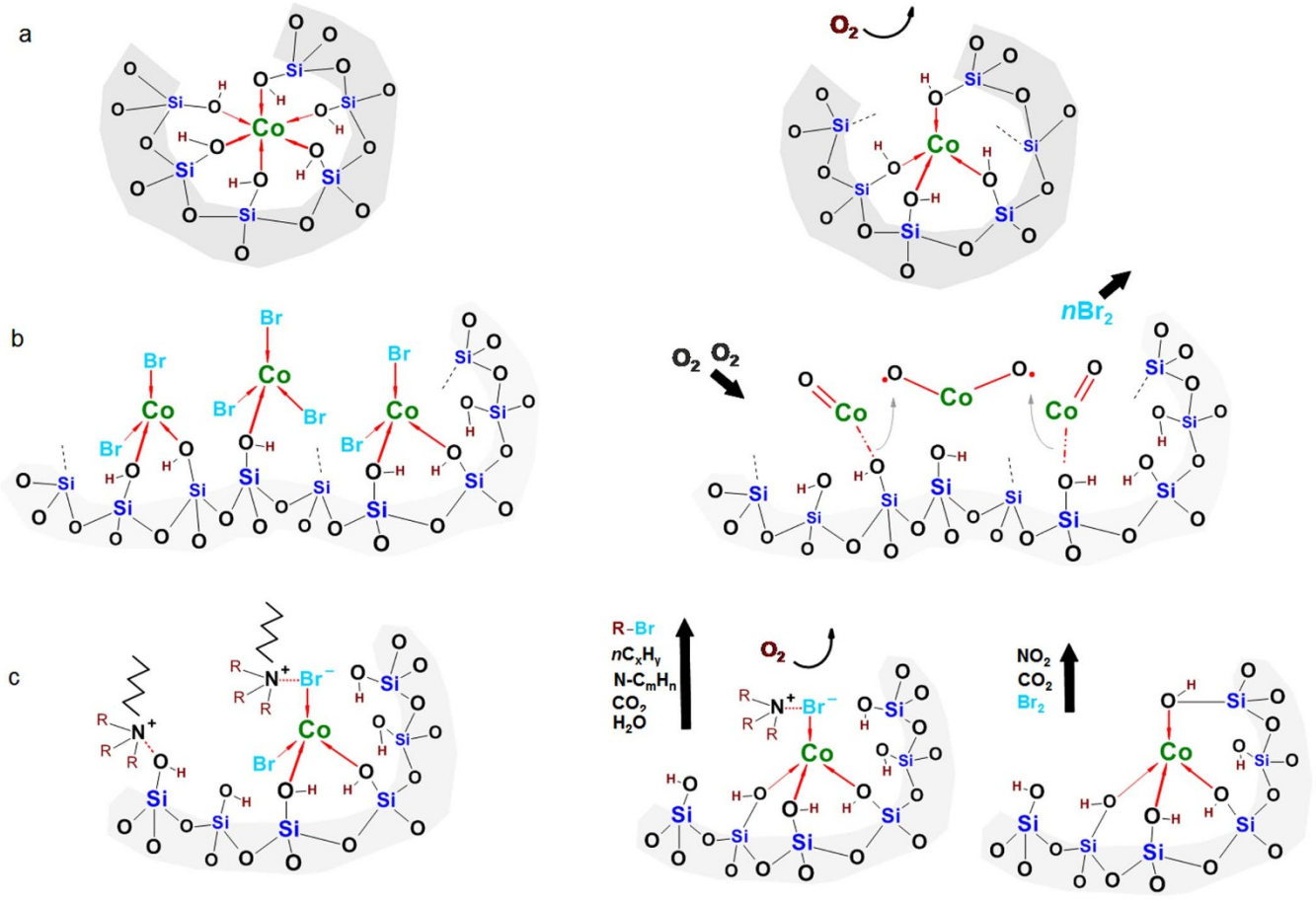

Figure 4 | Tailoring the oxidation state of cobalt through halide functionality inside a pore network. (a) Native cobalt silica (left) uncalcined material (right) calcined material; (b) Surfactant cobalt silica ($x < 1$) (left) uncalcined material (right) calcined material; (c) Surfactant cobalt silica ($x > 1$) (left) uncalcined material (middle) calcined material (< 400°C) (right) calcined material (> 500°C).

the presence of head groups strongly attached to the network beyond the typical decomposition temperature in pure silica surfactant materials. Therefore, we can infer that surfactant monomers (especially head groups) might create alternative interactions with either cobalt or Co-Br coordination in the early stages of material preparation, thereby undertaking an extended thermal decomposition during calcination. Therefore, this atypical metal-surfactant interaction may inhibit the oxidation process inside the silica matrix[30,31].

Discussion

The tailoring of the cobalt functionality in sol-gel derived silica in this work through the interactions with the cationic surfactant and its halide counter ions is elucidated in Fig. 4. For low concentrations of surfactant ($x \leq 1$) the complexation of the bromide counter ions with cobalt during the sol-gel synthesis leaves the surfactant, in particular the N^+ head group, to interact with surface silanols in the silica matrix. During calcination the cobalt bromide complex is more easily oxidized in comparison to the native cobalt silica due to the weaker tetragonal coordination of the cobalt bromide (Fig. 4 (a) and (b)). Meanwhile, the surfactant itself undergoes a separate decomposition process unrelated to the cobalt bromide, wherein an initial endothermic step is associated with Hofmann degradation (SI – Eq. 1) and is followed by further oxidation of the Hofmann byproducts below 400°C (SI – Eq. 2)[32].

As x approaches 1 the silica surface becomes saturated with surfactant species, with further addition of surfactant ($x > 1$) leading to the formation of mesoporous structures suggesting surfactant aggregation. In particular, the surfactant head group must interact with and aggregate around the cobalt bromide complex. This in turn inhibits the decomposition of the aliphatic tails via the Hofmann degradation, which instead occurs via a cracking pyrolysis mechanism (Fig. 4 (c) middle), as evidenced by the lack of endothermic peak at < 200°C, the decreased intensity of the narrow DTA peak at ~250°C and generation of new, broad exothermic DTA peaks at temperatures between 250 and 500°C. However, to inhibit Co_3O_4 formation, the surfactant head group/cobalt bromide interaction must remain strongly coordinated; hindering the oxidation process and preserving the Co^{2+} state in a similar manner to the native cobalt silica (Fig. 4 (c) right). That the head groups only start to decompose at ~535°C and then via an altered decomposition pathway (SI – Eq. 3), provides strong evidence for this enhanced interaction.

In summary, we have uncovered a new functionality of halides to control the oxidation state of cobalt particles embedded in silica matrices and a new method for enhancing the Co_3O_4 formation within silica has been successfully demonstrated. By complexing halide counter-ions from cationic surfactants with cobalt during the sol-gel synthesis, we were able to effectively double the functionality or oxidation state of the cobalt within the silica matrix, without altering the amount of cobalt precursor used. These results have significant implications for the production of cobalt/silica composites where maximizing the desirable Co_3O_4 phase remains the principal priority.

Method

In a typical synthesis, a master sol of cobalt silica was produced by dissolving cobalt nitrate hexahydrate ($Co(NO_3)_2.6H_2O$) in hydrogen peroxide (30 wt% in water) and mixing the resulting solution with ethanol (EtOH), followed by the drop wise addition of tetraethoxysilane (TEOS). The final molar ratios TEOS : H_2O : H_2O_2 : EtOH : $Co(NO_3)_2.6H_2O$ = 4 : 45.5 : 9 : 256 : 1[33]. The polymerization process is carried out in a controlled pH environment due to the above mentioned incorporation of peroxide. Hybrid surfactant cobalt silica sols were then synthesized preserving a fixed Co/Si molar ratio by adding hexyl triethyl ammonium bromide (HTAB) at molar ratios for HTAB: $Co(NO_3)_2.6H_2O$ (herein referred to as the surfactant/cobalt molar ratio) of 0.25 to 3, or equivalent to 0.47 to 5.4 wt%. The excess of ethanol provides the adequate conditions to work well below the micelle critical point of HTAB whilst preserving the surfactant solubility. The resultant homogeneous and stable hybrid sols (given the nomenclature SCoSi x, where x refers to the surfactant/cobalt molar ratio) were dried at 60°C for 96 hours and then calcined in air at 600°C (ramp rate of 1°C min^{-1} and a dwell time of 150 minutes) to create the final stable xerogels. Identification and quantification of the relevant silica functional groups and cobalt oxide phases was performed via Fourier transform infra-red spectrometry (FTIR) collected on a Shimadzu IRAffinity-1; diffusive reflection UV-Vis (DR-UV-Vis) spectrometry collected on a Varian spectrophotometer equipped with an integrating sphere; and X-ray Photoelectron Spectrometry (XPS) using Al Kα X-rays at 1486.6 eV (with the spectra adjusted to C at 284.6 eV). Qualification of the reaction products during thermal treatment was monitored by a Texas Instruments Q500 thermogravimetric analysis system linked to a ThermoStar mass spectrometer gas analysis system. Differential Thermal Analysis was undertaken with a Mettler Toledo TGA/DSC 1 Thermogravimetric Analyzer with GC200 Gas controller. TEM measurement was performed on a JEOL 1010 transmission electron microscope (TEM) operated at 100 kV. Structural data was collected from X-ray diffraction (XRD) using a Bruker D8 Advance diffractometer with a Cu Kα radiation (40 kV, 20 mA, λ = 1.5409A°).

1. Davis, M. E. Ordered porous materials for emerging applications. *Nature* **417**, 813–821 (2002).
2. Caruso, F., Caruso, R. A. & Mohwald, H. Nanoengineering of inorganic and hybrid hollow spheres by colloidal templating. *Science* **282**, 1111–1114 (1998).
3. Kanezashi, M., Yada, K., Yoshioka, T. & Tsuru, T. Organic-inorganic hybrid silica membranes with controlled silica network size: preparation and gas permeation characteristics. *J. Membr. Sci.* **348**, 310–318 (2010).
4. Cassiers, K. *et al.* A detailed study of thermal, hydrothermal, and mechanical stabilities of a wide range of surfactant assembled mesoporous silicas. *Chem. Mater.* **14**, 2317–2324 (2002).
5. Grosso, D. *et al.* Two-dimensional hexagonal mesoporous silica thin films prepared from black copolymers: Detailed characterization amd formation mechanism. *Chem. Mater.* **13**, 1848–1856 (2001).
6. Duke, M. C., Diniz da Costa, J. C., Do, D. D., Gray, P. G. & Lu, G. Q. Hydrothermally robust molecular sieve silica for wet gas separation. *Adv. Funct. Mater.* **16**, 1215–1220 (2006).
7. Martyanov, I. N., Uma, S., Rodrigues, S. & Klabunde, K. J. Decontamination of gaseous acetaldehyde over CoOx-loaded SiO_2 xerogels under ambient, dark conditions. *Langmuir* **21**, 2273–2280 (2005).
8. Yacou, C., Smart, S. & Diniz da Costa, J. C. Long term performance cobalt oxide silica membrane module for high temperature H_2 separation. *Energ. Environ. Sci.* **5**, 5820–5832 (2012).
9. Al-Badri, Z. M. *et al.* Room temperature magnetic materials from nanostructured diblock copolymers. *Nat. Commun.* **2**, (2011).
10. Mattei, G. *et al.* Synthesis, structure, and magnetic properties of Co, Ni, and Co-Ni alloy nanocluster-doped SiO_2 films by sol-gel processing. *Chem. Mater.* **14**, 3440–3447 (2002).
11. Khodakov, A. Y., Chu, W. & Fongarland, P. Advances in the development of novel cobalt Fischer-Tropsch catalysts for synthesis of long-chain hydrocarbons and clean fuels. *Chem. Rev.* **107**, 1692–1744 (2007).
12. Chen, J. F., Zhang, Y. R., Tan, L. & Zhang, Y. A simple method for preparing the highly dispersed supported Co_3O_4 on silica support. *Ind. Eng. Chem. Res.* **50**, 4212–4215 (2011).
13. Jia, C.-J. *et al.* Co_3O_4–SiO_2 nanocomposite: a very active catalyst for CO oxidation with unusual catalytic behavior. *J. Am. Chem. Soc.* **133**, 11279–11288 (2011).
14. Martínez, A. n., López, C., Márquez, F. & Díaz, I. Fischer–Tropsch synthesis of hydrocarbons over mesoporous Co/SBA-15 catalysts: the influence of metal loading, cobalt precursor, and promoters. *J. Catal.* **220**, 486–499 (2003).
15. Bourikas, K., Kordulis, C., Vakros, J. & Lycourghiotis, A. Adsorption of cobalt species on the interface, which is developed between aqueous solution and metal oxides used for the preparation of supported catalysts: a critical review. *Adv. Colloid Interface Sci.* **110**, 97–120 (2004).
16. Uhlmann, D., Smart, S. & Diniz da Costa, J. C. High temperature steam investigation of cobalt oxide silica membranes for gas separation. *Sep. Purif. Technol.* **76**, 171–178 (2010).
17. Miller, C. R., Wang, D. K., Smart, S. & Diniz da Costa, J. C. Reversible Redox Effect on Gas Permeation of Cobalt Doped Ethoxy Polysiloxane (ES40) Membranes. *Sci. Rep.* **3**, 1648; doi:10.1038/srep01648 (2013).
18. Riva, R., Miessner, H., Vitali, R. & Del Piero, G. Metal-support interaction in Co/SiO_2 and Co/TiO_2. *Appl. Catal. A-Gen.* **196**, 111–123 (2000).
19. Esposito, S. *et al.* Cobalt-silicon mixed oxide nanocomposites by modified sol-gel method. *J. Solid State Chem.* **180**, 3341–3350 (2007).
20. Che, S. *et al.* Synthesis and characterization of chiral mesoporous silica. *Nature* **429**, 281–284 (2004).
21. Inagaki, S., Guan, S., Ohsuna, T. & Terasaki, O. An ordered mesoporous organosilica hybrid material with a crystal-like wall structure. *Nature* **416**, 304–307 (2002).
22. Olejniczak, Z. *et al.* ^{29}Si MAS NMR and FTIR study of inorganic-organic hybrid gels. *J. Mol. Struct.* **744–747**, 465–471 (2005).
23. Ortega-Zarzosa, G., Araujo-Andrade, C., Compean-Jasso, M. E., Martinez, J. R. & Ruiz, F. Cobalt oxide/silica xerogels powders: X-ray diffraction, infrared and visible absorption studies. *J. Sol-Gel. Sci. Techn.* **24**, 23–29 (2002).
24. Okamoto, Y. *et al.* Preparation and characterisation of highly dispersed cobalt oxide and sulfide catalysts supported on SiO_2. *J. Phys. Chem.* **95**, 310–319 (1991).

25. Tan, B. J., Klabunde, K. J. & Sherwood, P. M. A. XPS studies of solvated metal atom dispersed catalysts - evidence for cobalt-manganese particles on alumina and silica. *J. Am. Chem. Soc.* **113**, 855–861 (1991).
26. Fine, D. A. Halide complexes of cobalt (II) in acetone solution. *J. Am. Chem. Soc.* **84**, 1139–1144 (1962).
27. Wertz, D. L. & Kruh, R. F. Solute-solvent interactions in some concentrated cobalt (II) bromide solutions. *Inorg. Chem.* **9**, 595–598 (1970).
28. Bobtelsky, M. & Spiegler, K. S. The cobalt halide and thiocyanate complexes in ethyl-alcoholic solution. *J. Chem. Soc.* 143–148 (1949).
29. Kleitz, F., Schmidt, W. & Schüth, F. Calcination behavior of different surfactant-templated mesostructured silica materials. *Micropor. Mesopor. Mat.* **65**, 1–29 (2003).
30. de Souza, L. K. C., Pardauil, J. J. R., Zamian, J. R., da Rocha, G. N. & da Costa, C. E. F. Influence of the incorporated metal on template removal from MCM-41 type mesoporous materials. *J. Therm. Anal. Calorim.* **106**, 355–361 (2011).
31. Goworek, J., Kierys, A., Gac, W., Borowka, A. & Kusak, R. Thermal degradation of CTAB in as-synthesized MCM-41. *J. Therm. Anal. Calorim.* **96**, 375–382 (2009).
32. Kleitz, F., Schmidt, W. & Schüth, F. Evolution of mesoporous materials during the calcination process: structural and chemical behavior. *Micropor. Mesopor. Mat.* **44–45**, 95–109 (2001).
33. Uhlmann, D., Liu, S., Ladewig, B. P. & Diniz da Costa, J. C. Cobalt-doped silica membranes for gas separation. *J. Membr. Sci.* **326**, 316–321 (2009).

Acknowledgments

The authors would like to acknowledge funding support from the Australian Research Council through Discovery Project Grant DP110101185. Gianni Olguin also acknowledges funding support from the bicentenary scholarship program from the Chilean Government. The authors gratefully acknowledge Dr Wayde Martens from the Queensland University of Technology for his assistance with the TGA/MS and the facilities, scientific and technical assistance of Dr Barry Wood of the Australian Microscopy & Microanalysis Research Facility at the Centre for Microscopy and Microanalysis, The University of Queensland.

Author contributions

G.O. performed the experiments and prepared the first draft of the manuscript including all the figures and supplementary information. S.S., C.Y. and J.C.D.C. contributed to the analysis and discussion of the results and the final writing process. All authors wrote, read and corrected the final manuscript before submission.

Additional information

Supplementary information accompanies this paper at http://www.nature.com/scientificreports

Competing financial interests: The authors declare no competing financial interests.

How to cite this article: Olguin, G., Yacou, C., Smart, S. & Diniz da Costa, J.C. Tailoring the oxidation state of cobalt through halide functionality in sol-gel silica. *Sci. Rep.* **3**, 2449; DOI:10.1038/srep02449 (2013).